Thermo-responsive lamellar hydrogels with tunable turbidity, structural color, and anisotropic swelling

Yang Han [a], *Yunzhou Guo*[ab], *Tasuku Nakajima*[cd*] *and Jian Ping Gong*[cd*]

[a] Graduate School of Life Science, Hokkaido University, Sapporo 001-0021, Japan; [b] ZJU-Hangzhou Global Scientific and Technological Innovation Center, Zhejiang University, Hangzhou 311215, China; [c] Institute for Chemical Reaction Design and Discovery (WPI-ICReDD), Hokkaido University, Sapporo 001-0021, Japan; [d] Faculty of Advanced Life Science, Hokkaido University, Sapporo 001-0021, Japan

KEYWORDS: anisotropic hydrogel, thermo-responsivity, phonic material, structural color, smart window

ABSTRACT: We report a thermo-responsive anisotropic photonic hydrogel: poly(dodecyl glyceryl itaconate)/polyacrylamide-poly(*N*-isopropylacrylamide) hydrogel (PDGI/PAAm-PNIPAM hydrogel). Hydrogels with uniaxially aligned lamellar bilayers possess bright structural color and swelling anisotropy, while PNIPAM-based hydrogels exhibit distinct thermo-responsive properties around a lower critical solution temperature (LCST). Hybridization of thermo-responsive PNIPAM with the lamellar hydrogel can give the anisotropic photonic hydrogel with various fascinating thermo-responsive properties, such as structural color/turbid transition,

thermo-responsive structural color, and anisotropic deswelling/reswelling behavior by temperature stimuli. The temperature-induced change in turbidity, structural color, and anisotropic swelling of the gel around LCST can be tuned by controlling the incorporated PNIPAM density. PNIPAM can be regioselectively incorporated into the specific region of the lamellar hydrogels by photomasking during UV polymerization. The PDGI/PAAm-PNIPAM hydrogel can find diverse promising applications, such as smart windows and smart displays.

1. INTRODUCTION

Nowadays, the drastic development of thermo-responsive polymer-based smart materials has been aroused due to their unique functionalities.[1] The most well-known and extensively researched thermo-responsive polymeric systems are aqueous poly(*N*-isopropylacrylamide) (PNIPAM) and its derivatives.[2-7] Aqueous PNIPAM is classified as lower critical solution temperature (LCST)-type thermo-responsive material, which is hydrophilic below LCST but becomes hydrophobic above LCST through dehydration.[5-7] This hydrophilic/hydrophobic transition at LCST imparts unprecedented properties to PNIPAM-based smart aqueous materials. For example, PNIPAM-based hydrogels exhibit transparent/turbid transition associated with the swelling/shrinking behavior upon heating and cooling process, enabling various promising applications, such as optical applications in thermo-responsive smart windows and biomedical applications in drug delivery.[2,5]

On the other hand, recently hydrogels with periodically oriented two-dimensional (2-D) materials have been developed so far.[8-11] Examples include hydrogels with aligned clay nanosheets,[11-13] hydrogels with stacked inorganic nanosheets,[14,15] and hydrogels with monodomain

lamellar bilayers.[16-19] Such a new class of hydrogels holds great promise as anisotropic structural materials, actuators with directional movements, and bright photonic gels owing to periodic assembly of the 2-D materials.[16,17] Among them, our group has developed an anisotropic lamellar hydrogel by entrapping thousands of self-assembled poly(dodecyl glyceryl itaconate) (PDGI) lipid bilayers inside a soft polyacrylamide (PAAm) network.[18-21] The rigid and water-impermeable PDGI bilayers form a monodomain lamellar structure with a spacing of ~100 nm in the gel through the shear-flow induced self-assembly. The resulting PDGI/PAAm hydrogels with monodomain lamellar structure possess various unique properties, such as bright and tunable structure color owing to the periodic lamellar structure, high toughness owing to the rigid bilayers as sacrificial bonds, and distinct one-dimensional swelling in perpendicular to bilayer direction owing to the macroscopic orientation of the rigid bilayers.

Attempts have been made to incorporate thermo-responsive polymers into such hydrogels with 2-D materials to introduce a unique thermal response to the anisotropic hydrogels.[2,11-16,22] Departing from conventional isotropic thermo-responsive hydrogels, the incorporation of thermo-responsive polymers into the anisotropic hydrogels with 2-D materials holds the potential to introduce unique functionalities and properties. For example, Miyamoto *et al.* reported the anisotropic PNIPAM hydrogel by utilizing the inorganic nanosheet liquid crystals (LCs).[14] This anisotropic hydrogel was synthesized by radical polymerization of NIPAM in the presence of inorganic nanosheet LCs by using shear force-induced orientation. The multicomponent gels with anisotropic structure exhibit thermo-responsive anisotropic swelling and may find applications in soft actuators and sensors. Aida *et al.* developed a PNIPAM-based smart hydrogel with oriented unilamellar titanate(IV) nanosheets (TiNS), which could undergo anisotropic deformations as a consequence of the contraction and expansion of the cofacial TiNS distance triggered by

temperature.[22] In contrast to conventional PNIPAM-based hydrogels that show homogeneous swelling/deswelling, the thermal behavior of their hydrogel, containing cofacial TiNSs, could not only be opposite (heating-induced swelling and cooling-induced shrinking) but also anisotropic. These innovations, stemming from the synergy of thermo-responsiveness and anisotropic structures, could open up a new chapter in material science.

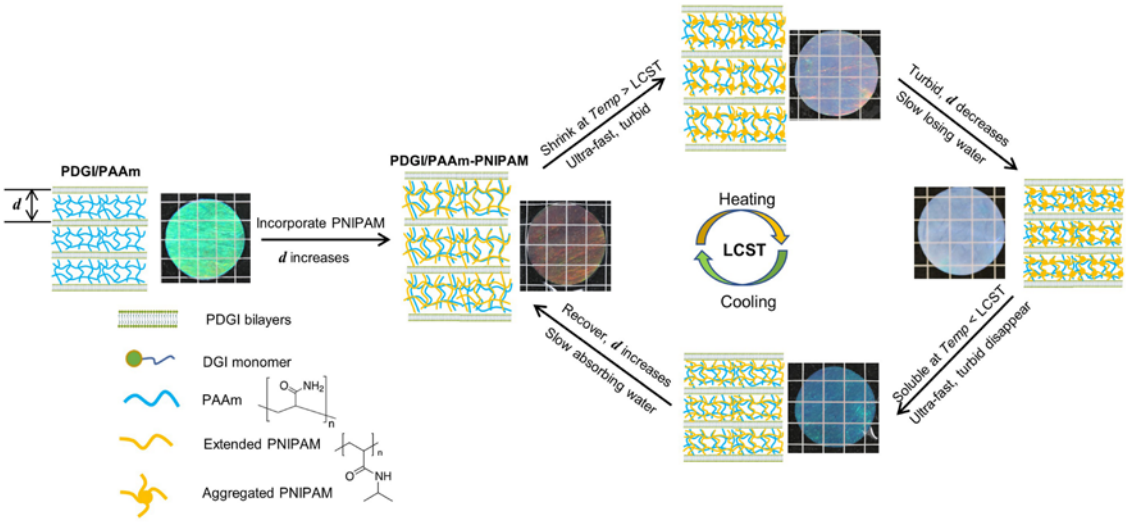

Scheme 1. Illustration of the thermo-responsive anisotropic photonic hydrogel, PDGI/PAAm-PNIPAM hydrogel. This hybrid hydrogel has a hard, anisotropic PDGI bilayer and a soft, thermo-responsive PAAm-PNIPAM layer. When the temperature (*Temp*) is higher than the lower critical solution temperature (LCST) of PNIPAM, the PNIPAM network becomes hydrophobic, and the gel becomes turbid immediately and releases water gradually. With the water release, the gel mainly shrinks along the thickness direction owing to the presence of macroscopic bilayers, and the interplanar distance of the gel decreases gradually, leading change in the structural color. At *Temp* < LCST, PNIPAM becomes hydrophilic and the turbidity disappears immediately. The interplanar distance of the gel increases gradually absorbing water to reach the original/swollen state.

In this work, we incorporate PNIPAM as the thermo-responsive component into PDGI/PAAm lamellar hydrogels to form PDGI/PAAm-PNIPAM hydrogels with unique thermo-responsive optical and swelling properties. PNIPAM is incorporated into the PAAm layer of PDGI/PAAm hydrogels to form an interpenetrating soft layer of PAAm-PNIPAM (Scheme 1) inside the hydrogels while maintaining the anisotropic structure. As introduced above, aqueous PNIPAM undergoes a temperature-driven, reversible LCST-type phase transition. Below the LCST, it is water-soluble owing to strong hydrogen bonds between the amide groups and the water molecules. Above the LCST, weakened hydrogen bonds and strengthened hydrophobic interactions instantly make the PNIPAM chains contract into hydrophobic globules, making the system turbid.[2,23-26] Introduction of a thermo-responsive PNIPAM network into the hydrophilic PAAm to form an interpenetrating network negligibly affects the phase separation and LCST of PNIPAM, suggesting a negligible effect of the PNIPAM-PAAm interaction on the phase separation.[27] As a consequence, after the introduction of the PNIPAM network into the lamellar hydrogels, turbidity of such photonic PDGI/PAAm-PNIPAM hydrogels can be instantly tuned with temperature, leading to a structural color/turbid transition of the gel at LCST. Moreover, the PDGI/PAAm-PNIPAM hydrogels exhibit quasi 1-D swelling/deswelling by temperature stimuli around LCST, making the structural color tunable by temperature. The effect of incorporated PNIPAM density on the properties of the hydrogel has also been investigated, including turbidity, swelling anisotropy, structural color tunability, and their reversibility.

2. EXPERIMENTAL SECTION

2.1 Materials. An amphiphilic monomer, dodecyl glyceryl itaconate [DGI (*n*-$C_{12}H_{25}$-$OCOCH_2C$-$(=CH_2)COOCH_2CH(OH)CH_2OH$)], was synthesized following the procedure

described earlier.[28] After completion of the synthesis of DGI, the crude product was purified at least twice by a silica gel column (silica gel 60 N, Kanto Chemical Co., Inc., Japan). The DGI fraction was eluted with a hexane/ethyl acetate mixture (1:1 by volume) and was further purified twice by recrystallization from an acetone/hexane mixture (1/1 by weight). *N*,*N*′-Methylenebis(acrylamide) (MBAA, 99.0%, FUJIFILM Wako Pure Chemical Corporation, Japan) was recrystallized from ethanol, acrylamide (AAm, 98%, JUNSEI Chemicals Co. Ltd., Japan) was recrystallized from chloroform, and *N*-isopropylacrylamide (NIPAM, 97%, Sigma-Aldrich Co., USA) was recrystallized twice from a diethyl ether/hexane mixture. 2-Hydroxy-4′-(2-hydroxyethoxy)-2-methylpropiophenone (Irgacure 2959, 98%, Sigma-Aldrich Co., USA) and sodium dodecyl sulfate (SDS, 98%, FUJIFILM Wako Pure Chemical Corporation, Japan) were used as received. Milli-Q deionized water was used to prepare the monomer solutions and for the swelling of the gels.

2.2 Gel Preparation. The PDGI/PAAm-PNIPAM hydrogels were prepared in two steps. First, PDGI/PAAm hydrogels were prepared by simultaneous free-radical polymerization from an aqueous solution of 0.10 M DGI, 0.025 mM SDS, 4 M AAm, 4 mM MBAA as a cross-linker of AAm, and 2 mM Irgacure 2959 as a photoinitiator. The detailed procedure was described in our previous papers.[18,20,29] In short, a glass bottle with a mixture of the precursors and water was allowed to stand in a 55 °C (above Krafft point of DGI at 43 °C) water bath for 10 min and apply gentle shear to the mixture to dissolve DGI powders. Then the solution was kept again in a 55 °C water bath for 5 h to form stable lamellar bilayers of self-assembled DGI with trace SDS. Then the solution was transferred to a glove box filled with argon to remove dissolved oxygen in the solution. A sheet-like PDGI/PAAm hydrogel ($15 \times 7 \times 0.5$ cm^3) with a monodomain multilamellar structure parallel to the sheet surface was achieved following the same procedure described in our previous

paper.[30] Briefly, before the polymerization, we poured the precursor solution into the glass substrate with a shear flow to align thousands of lamellar bilayers of self-assembled DGI parallel to the surface of the glass substrate. After UV polymerization of DGI and AAm, bilayers of polymerized PDGI were entrapped in the PAAm matrix to give an anisotropic and mechanically tough hydrogel. After attaining swelling equilibrium in water, a greenish PDGI/PAAm gel was obtained.

In the second step, the greenish PDGI/PAAm gel was immersed in an aqueous solution of *c* M NIPAM, 0.05 mM MBAA, and 0.05 mM Irgacure 2959 for 7 days. *c* is called the feed concentration of NIPAM of the precursor solution. *c* was set to 0, 0.25, 0.5, and 1.0 M considering the highest solubility of NIPAM in water at room temperature. During solvent exchange from pure water to the NIPAM solution, a large shrinkage in thickness of the gel as well as a blue-shift of the structural color were observed probably because NIPAM aqueous solution is a relatively poor solvent for the gel, causing the gel to lose water. By performing a second UV polymerization of NIPAM in the presence of the PDGI/PAAm gel at 4 °C for 8 h, the PNIPAM network was formed within the PAAm network and an interpenetrating network structure was constructed. The obtained gels are coded as PDGI/PAAm-PNIPAM$_{c\mathrm{M}}$ hydrogel.

As a control, a PAAm-PNIPAM interpenetrating network gel without PDGI bilayers was prepared by incorporating the PNIPAM into the PAAm network. The PAAm network was synthesized by 4 M AAm, 4 mM MBAA as a cross-linker of AAm, and 2 mM Irgacure 2959 as an initiator. The incorporation of the PNIPAM network follows the same way as mentioned above.

2.3 Reflection spectrum measurement. Reflection spectra of various gel samples were measured by a combined setup of a light source, variable angle measurement device, and an analyzer. An Xe lamp was used as a light source to obtain the reflection spectrum. Reflection

measurement optics with variable angles (Hamamatsu Photonics KK, C10027A10687) were used to detect the reflected light. A photonic multichannel analyzer (Hamamatsu Photonics KK, C10027) was used for analyzing the detected signals. The entire reflection spectrum was obtained by keeping the incident angle at 60° and reflection angles at 45°. The distance between two lamellar layers, *d*, was roughly calculated using Bragg's law of diffraction, $\lambda_{max} = 2nd\sin\theta$, where $n = 1.33$ is the refractive index of water, θ is the incident angle, and λ_{max} is the wavelength at maximum reflectance intensity.[29]

2.4 Polarized optical microscope observation. The anisotropic structure of gels was observed by the polarized optical microscope (POM, Nikon Eclipse LV100POL) under crossed Nicol at 25°C. A tint plate (530 nm) was used to examine the orientation direction. The observation was performed from the top surface (top view) and the cross-section (side view) of the sheet-like gels. Before the observation, the gel sample was cut into a rectangular sheet (~50 x 2 x 1.2 mm^3 for the top view and ~30 x 1 x 1.2 mm^3 for the side view).

2.5 Water content measurement. The water content of the gel was measured using a moisture balance MOC-120H (Shimadzu Co.). The wet samples were heated at 120 °C until complete drying.

2.6 Swelling Ratio Measurement. For the swelling experiment, a swollen gel was cut into a cylindrical shape using a cylinder cutter (Diameter = 20.0 mm). The diameter of a cylindrical gel at different swollen states, *D*, was measured by a slide caliper. The thickness of the PDGI/PAAm and PDGI/PAAm-PNIPAM gels, *T*, was measured using a mechanical thickness meter (Teclck, Dumb Bell Ltd., Japan), and the thickness of the PAAm-PNIPAM gels was measured by Keyence laser thickness mater (CL-L015N, Keyence Corporation, Japan).

2.7 Thermal Analysis. The lower critical solution temperature (LCST) of PDGI/PAAm-PNIPAM hydrogels was measured using a differential scanning calorimeter (DSC 2500, TA instrument, USA) under a nitrogen atmosphere. The heating rate was 3 ^{o}C min^{-1}. The temperature at which phase transition occurs, LCST, was measured as the peak temperature of an exothermic reaction.

2.8 Transmittance Analysis. The transmittance of the sample was measured using an ultraviolet/visible light spectrophotometer (UV-1800, SHIMADZU, Japan) with a temperature control device. A sheet-like gel sample was placed in a quartz cuvette filled with water during measurement. The light was imposed on the top surface of the gel. The transmittance spectra of the samples in the range of 400–700 nm were measured.

3. RESULTS AND DISCUSSION

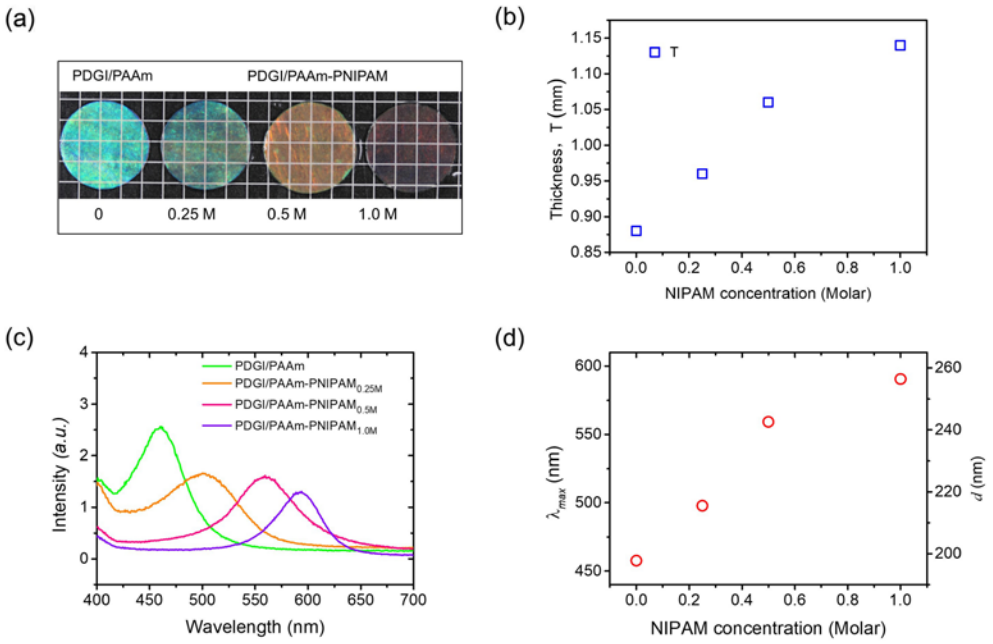

Figure 1. (a) Photographs, (b) thickness, *T*, and (c) reflection spectra of PDGI/PAAm and PDGI/PAAm-PNIPAM hydrogels synthesized with different NIPAM feed concentration in pure water at room temperature; (d) Peak wavelength, λ_{max}, of the reflection spectrum and the corresponding interplanar distance, *d*, as a function of NIPAM concentration.

3.1 Effect of NIPAM concentration on gel color. Lamellar PDGI/PAAm-PNIPAM hydrogels were successfully synthesized as described in the experimental section. The formation of PNIPAM in the PDGI/PAAm hydrogel was supported by the differential scanning calorimetry (DSC) results. The incorporation of PNIPAM networks into the PAAm soft layers makes PDGI/PAAm-PNIPAM hydrogels temperature-responsive with LCST around temperature (*Temp*) = 35 ℃ (Figure S1). The presence of the PAAm and PDGI does not appear to affect the phase separation behavior of PNIPAM in the gels.

We tuned PNIPAM density in the PDGI/PAAm-PNIPAM hydrogels by controlling the NIPAM feed concentration of the precursor solution for PNIPAM, *c*, as a parameter. We coded the obtained gels as PDGI/PAAm-PNIPAM$_{cM}$ hydrogels. Photographs of the PDGI/PAAm and PDGI/PAAm-PNIPAM hydrogels in swelling equilibrium at *Temp* = 25 °C are shown in Figure 1a. The diameter of the gels has been configured to 20 mm using a cylinder cutter. The PDGI/PAAm gels exhibited a green structural color. The PDGI/PAAm-PNIPAM gels also exhibited bright structural color like the PDGI/PAAm gels, suggesting the periodic PDGI lamellar structure was preserved even after incorporation of PNIPAM, while their structural color was tunable by the NIPAM feed concentration, *c*. At low *c* (PDGI/PAAm-PNIPAM$_{0.25M}$), the color of the gels slightly shifted to a green-orange color. With increasing *c*, the color of the gel changed to red (PDGI/PAAm-PNIPAM$_{0.5M}$) or dark red (PDGI/PAAm-PNIPAM$_{1.0M}$). The water content of the green PDGI/PAAm gel and red PDGI/PAAm-PNIPAM$_{0.5M}$ gel at 25 ºC were 90.3 and 92.0 wt%, respectively. The red shift in structural color of the PDGI/PAAm-PNIPAM gels accompanies an increase in the swelling ratio with increasing *c* (Figure 1b). Here, we observed remarkable swelling along the thickness direction but negligible swelling along the radial direction after incorporation of PNIPAM because the rigid PDGI lamellar bilayers restrict the in-plane swelling, which is discussed later in detail.[20]

The reflection spectra of the PDGI/PAAm-PNIPAM hydrogels with different *c* are shown in Figure 1c. The reflection spectra showed a red shift of the reflection peak in accordance with the color shift of the gels with increasing *c*. The peak wavelength, λ_{max}, was extracted from the reflection spectra, and the distance between two lamellar layers, *d*, was estimated from λ_{max} according to Bragg's equation (Figure 1d). λ_{max} of the PDGI/PAAm gel with green color was around 458 nm. After incorporating PNIPAM networks into PAAm soft layers, the λ_{max} increased

from 458 nm to 591 nm with an increase in *c* from 0 to 1.0 M. Therefore, tuning of the structural color of the PDGI/PAAm-PNIPAM gels corresponding to a wavelength shift of 133 nm can be achieved by controlling the NIPAM concentration. The red shift in the reflection spectrum of the PDGI/PAAm-PNIPAM gels is the result of the swelling of the gels along the thickness direction with increasing NIPAM concentration. The synthesized PNIPAM network forms an interpenetrating soft layer with PAAm in the PDGI/PAAm-PNIPAM hydrogels, which leads to an increase in osmotic pressure of the soft layers, resulting in an increased equilibrium swelling ratio of the gels.[31-33] The larger NIPAM concentration (the denser PNIPAM in the gel) leads to higher osmotic pressure, which promotes swelling more.

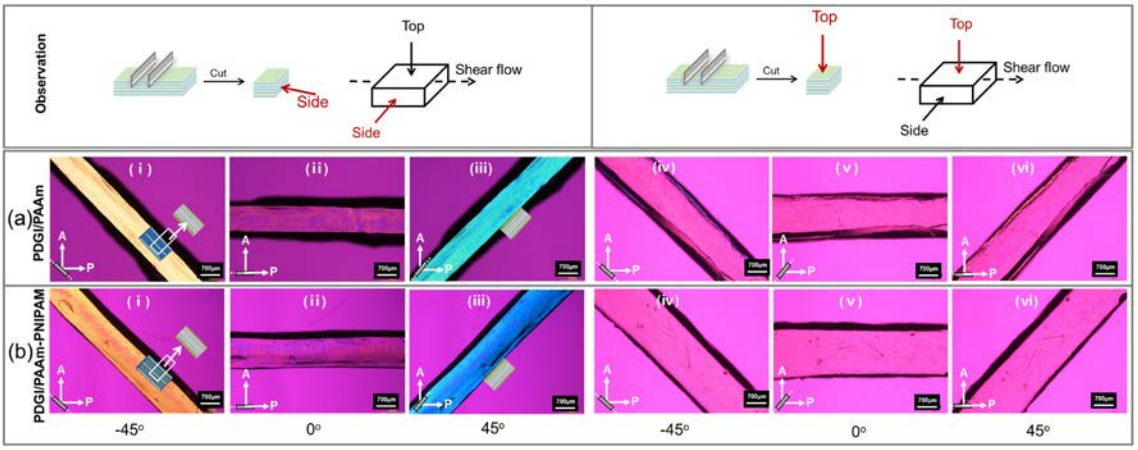

Figure 2. Polarizing optical microscope (POM) images of the fully swollen (a) PDGI/PAAm and (b) PDGI/PAAm-PNIPAM$_{0.5M}$ hydrogels in water at *Temp* = 25°C. The sample setup and observation directions are also shown. All the images are taken under cross-polarizers in the presence of a tint plate (530 nm). The scale bars are 700 μm.

3.2 Characterization of the anisotropic structure of the gel. Polarizing optical microscopy (POM) images were captured to justify the structural anisotropy of the PDGI/PAAm and PDGI/PAAm-PNIPAM$_{0.5M}$ lamellar hydrogels swollen in water at *Temp* = 25 °C (Figure 2). The

sample setup and observation directions are shown in the Figure. All the images were taken under cross-polarizers in the presence of a tint plate (530 nm). The PDGI/PAAm hydrogel exhibited strong birefringence, which has been assigned to the aligned monodomain bilayers and elongated PAAm chains along the direction perpendicular to the PDGI bilayers on account of the anisotropic swelling.[30] The PDGI/PAAm-PNIPAM$_{0.5M}$ gel with the incorporated PNIPAM network also exhibited strong birefringence. As shown in Figure 2a(i-iii) and 2b(i-iii), images of the cross-section of the PDGI/PAAm and PDGI/PAAm-PNIPAM$_{0.5M}$ lamellar gel (side) appeared orange at −45°(i), magenta at 0° (ii), and blue at +45°(iii) rotations relative to the polarizer, respectively. These results indicate that incorporating PNIPAM networks into PAAm layers does not affect the anisotropic swelling behavior along the thickness direction of the lamellar hydrogel. The monodomain PDGI bilayers in the gel, which govern the swelling anisotropy, barely got damaged after incorporating 0.5 M PNIPAM networks into PAAm layers, corresponding to the highly anisotropic swelling behaviors.

Top-view POM images of these lamellar gels showed no birefringence color at any rotation angle, confirming the isotropic in-plane structure of the lamellar bilayers (Figure 2a, b(iv-vi)).

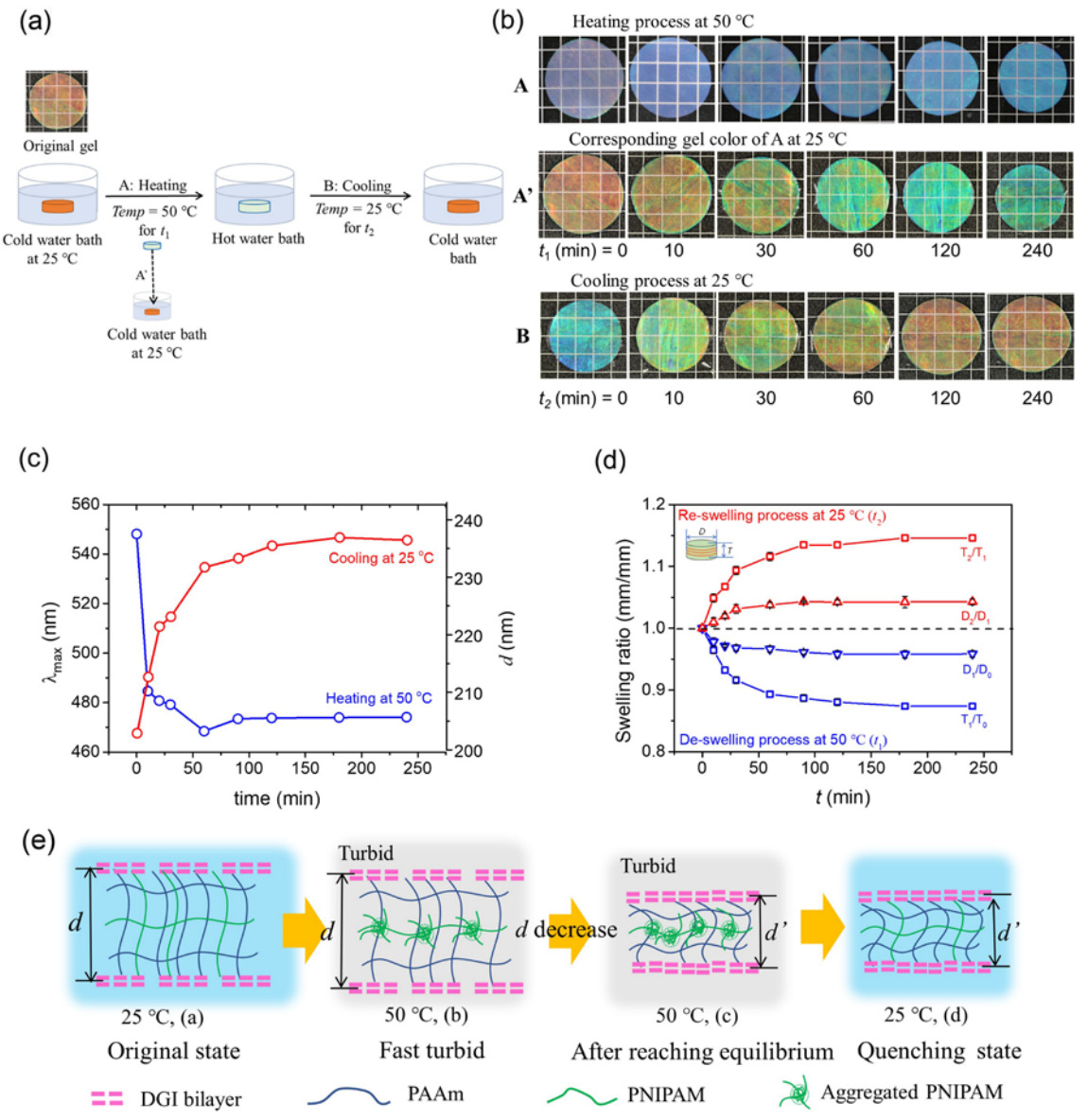

Figure 3. Deswelling/reswelling behaviors of the PDGI/PAAm-PNIPAM hydrogels during the heating and cooling process. (a) Experimental illustration for heating (for desired t_1) and cooling (for desired t_2) process, (b) optical images, (c) peak wavelength, λ_{max}, of the reflection spectrum and the corresponding interplanar distance, *d*, and (d) deswelling and reswelling ratios in water as a function of time during heating and cooling process. The corresponding color of the turbid gel, A', during t_1 was captured immediately after quenching the gel of A in a cold bath (*Temp* = 25 °C).

λ_{max} in (c) is measured using A' samples for the heating process. Background lattices in (a) and (b): 5 × 5 mm. (e) Illustration of the thermal-responsively turbid phenomenon of PDGI/PAAm-PNIPAM hydrogel based on the lamellar structure during the heating process.

3.3 The unique properties of the gel derived from thermo-responsive properties and anisotropic structure. In this section, the unique properties of the PDGI/PAAm-PNIPAM hydrogels derived from their thermo-responsivity and anisotropic structure are discussed. The obtained PDGI/PAAm-PNIPAM gels exhibit unique thermo-responsive visual and size changes. As a typical example, the results of the PDGI/PAAm-PNIPAM$_{0.5M}$ gel as the model gel are shown here.

We first show the thermo-induced ultra-fast structural color/turbid transition of the PDGI/PAAm-PNIPAM$_{0.5M}$ hydrogels (diameter = 20 mm, thickness ~ 1.0 mm) during the heating and cooling process across LCST. The gel exhibited structural color at 25 °C but instantly turned turbid when immersed into the 50 °C hot water bath owing to the hydrophobic association of the PNIPAM chains in the gel. It is worth mentioning that the turbidity of the heated gel is controllable by the heating temperature (Figure S2, S3, and Video S1, S2, S3).[34-36] When the heated gel was suddenly cooled to 25 °C, the turbidity disappeared immediately due to the recovery of hydrophilicity of the PNIPAM chains.[23] Timescale of the transparent/turbid transition was ~1 s. Note that the ultrafast transparent/turbid transition of the aqueous PNIPAM-based smart materials is general. Unlike typical temperature-responsive smart materials, which are colorless at low temperatures,[2] in this work, we utilized hydrogels with bright structural color as the base material to realize structural color/turbid transition. The colorful gels immediately turn into monochrome gels just by heating, which could be called the thermo-induced color/monochrome transition.

We then investigated the long-term thermo-responsive behaviors of the PDGI/PAAm-$PNIPAM_{0.5M}$ hydrogels during the heating and cooling process across LCST, including gradual structural color change and anisotropic deswelling/reswelling (Figure 3). The experimental process is shown in Figure 3a. The PDGI/PAAm-$PNIPAM_{0.5M}$ hydrogel at swelling equilibrium in a 25 ℃ cold water bath showed a red color. The red gel was then immersed into a 50 ℃ hot water bath for the time t_1. Pictures of the gels being heated at 50 ℃ for varied t_1 are shown in Figure 3b(A). The turbidity of the gel does not decay with time during heating (Figure 3b(A) and Figure S4), which is in accord with the LCST-type gels where the turbidity is mainly determined by the temperature but independent of time.[34-36] On the other hand, the gel gradually expelled water to deswell with time due to the hydrophobicity of PNIPAM.

Deswelling of the lamellar gels leads change of their structure color hidden by the turbidity. To investigate the hidden structural color of the PDGI/PAAm-$PNIPAM_{0.5M}$ gel during heating, the gel heated for the desired time t_1 was quenched by immersion into a 25 ℃ cold water bath. After the immediate disappearance of the turbidity of the gel, the instantaneous structural color of the gel was captured immediately. The quenched gel showed a t_1-dependent blue shift in the structural color (Figure 3b, A'). The color of the quenched gel gradually changed from red to green with the increase of t_1. At $t_1 > 2$ h, the gel showed no further structural color change. The reflection spectra also show a blue shift in peak wavelength, λ_{max}, from higher (~548 nm) to lower (~465 nm) wavelength in accordance with the blue shift in color with the increase of t_1 (Figure 3c and S5a). This indicates that the gel reached the new equilibrium state at 50 ℃ after 2 h heating at this condition. It should be noticed that bluish color was glimpsed in the turbid gel (Figure 3b(A)) independent of its hidden structural color (Figure 3b(A')). This is probably due to Rayleigh and Mie scatterings of aggregated PNIPAM in the gel. During heating at *Temp* > LCST, the PNIPAM

polymer chains within the networks undergo collapse and aggregation, leading to the formation of micro- or nanoscale structures that scatter light according to Rayleigh and Mie scattering theories.[37]

When the quenched gel was continuously immersed in a 25 ℃ cold water bath, the gel gradually reswelled to recover the original structural color as well as the original λ_{max} (~548 nm) and d (~ 237 nm) (Figure 3b(B) and 3c). λ_{max} and d decrease/increase accordingly during the heating/cooling processes. We immersed the gel equilibrated at 50 ℃ into a 25 ℃ cold water bath for the reswelling time t_2 and obtained the reflection spectra and corresponding d. Figure 3c and S5b show the change of d and the reflection spectra of the gel, respectively, with different reswelling times t_2. The increase in d during recovery is on account of the reswelling of the PAAm-PNIPAM soft layer at *Temp* < LCST.[2] This indicates that the thermal-induced structural color change of the gel is reversible.

We also measured the thermo-induced anisotropic deswelling/reswelling of the gel during the heating and cooling process (Figure 3d). Here, we set the PDGI/PAAm-PNIPAM$_{0.5M}$ hydrogel swollen in 25 ℃ cold water as the reference state, and the diameter and thickness of the gel at this state were set as D_0 and T_0. The gel was then heated at *Temp* = 50 ℃ for t_1. The diameter and thickness of the gel at this stage are shown as $D_1(t_1)$ and $T_1(t_1)$, and those at the new shrunken equilibrium state are shown as D_1 and T_1. The gel at the new shrunken equilibrium state was then quenched and kept in 25 ℃ cold water for t_2 to reswell. The diameter and thickness of the gel at reswelling time t_2 are shown as $D_2(t_2)$ and $T_2(t_2)$, and at fully recovered state as D_2 and T_2, respectively. The deswelling ratio of the cylindrical gel in the thickness direction (perpendicular to the PDGI bilayer) and diameter direction (parallel to the PDGI bilayer) were defined as $T_1(t_1)/T_0$ and $D_1(t_1)/D_0$, respectively. Similarly, the reswelling ratio of the gel in the thickness and diameter

directions are $T_2(t_2)/T_1$ and $D_2(t_2)/D_1$, respectively. Since the PDGI lipid bilayers in the PDGI/PAAm hydrogels are almost water impermeable and without any in-plane anisotropy,[18-21] the thermal-induced deswelling/reswelling of the gel is considered to only occur in the PAAm-PNIPAM soft layers. As shown in Figure 3d, the deswelling ratio of the PDGI/PAAm-PNIPAM$_{0.5M}$ hydrogel in the thickness direction ($T_1(t_1)/T_0$) decreased to 0.85 with increasing heating time t_1. On the other hand, only a slight decrease ($D_1(t_1)/D_0 \sim 0.95$) in the diameter direction is observed. For the cooling process, the gel fully recovered its original size ($T_2/T_1 \approx 1.15$, $D_2/D_1 \approx 1.04$) after 2 h immersion in 25 ℃ cold water. These indicate that the PDGI/PAAm-PNIPAM hydrogel shows reversible thermal-induced deswelling/reswelling behaviors with significant anisotropy. The PAAm-PNIPAM soft layers in PDGI/PAAm-PNIPAM gels mainly shrink/swell perpendicular to the bilayer direction under thermal stimuli, in contrast to isotropic deswelling/reswelling of typical PNIPAM-based hydrogels. For example, the PAAm-PNIPAM$_{0.5M}$ isotropic interpenetrating hydrogel without PDGI bilayers does not exhibit such swelling anisotropy during the heating and cooling process (Figure S6). Since PDGI lipid bilayers can be deemed as unexpandable stiff sheets, in-plain swelling/deswelling of the gel is restricted because such swelling must accompany the expansion of stiff sheets. This causes anisotropic deswelling of the gel along the thickness direction and a remarkable decrease in the interplanar distance as well as the blue shift of the structural color of the gel upon heating.[18-21]

The time difference for ultrafast structural color/turbid phenomenon (<1 s) and swelling process (~2 h) is discussed. An illustration to explain the cause of the difference is shown in Figure 3e. The original PDGI/PAAm-PNIPAM$_{0.5M}$ hydrogel turns turbid immediately after immersing in hot water and the turbidity disappears immediately after quenching the gel into cold water. This is because the PNIPAM-based lamellar gel exhibits immediate microphase separation same as

typical PNIPAM aqueous systems at *Temp* > LCST.[2] Once the gel is immersed in hot water, the PNIPAM network instantly becomes hydrophobic and aggregates together, resulting in the turbidity of the gel. Such hydrophobicity of PNIPAM also causes deswelling of the gel. Since deswelling requires long-path diffusion of water molecules, the timescale of diffusion of water for deswelling is much longer than that of the phase separation. In the case of the gels with the water-impermeable monodomain PDGI bilayers, the diffusion of water into and out of the hydrogel occurs mainly along the radial direction.[37] Timescale of water diffusion in the gel along this path can be estimated by the equation for 2-D diffusion, $t = L^2/4D_w$, where t is diffusion timescale, L is the length of the diffusion path, and D_w is the diffusion coefficient of water.[39,40] We roughly assume that D_w in the PDGI/PAAm-PNIPAM gel is the same as that of free water. By substitution of L = 1 cm (radius of the cylindrical gel) and $D_w = 3.983 \times 10^{-5}$ cm^2 s^{-1} at 50 ℃, the timescale of deswelling (t_{ds}) becomes 1.74 h. It indicates that the time for PDGI/PAAm-PNIPAM$_{0.5M}$ hydrogel to reach shrunken equilibrium at 50 ℃ is 1.74 h. While that for reswelling at 25 ℃, $D_w = 2.299 \times 10^{-5}$ cm^2 s^{-1}.[39] Therefore, the timescale of reswelling (t_{rs}) for the shrunken hydrogel to recover original state becomes 3.02 h. These estimations are in agreement with the experimentally observed deswelling/reswelling timescales.

In short summary, the PDGI/PAAm-PNIPAM hydrogels exhibit ultrafast structural color/turbid transition, gradual structural color change, and anisotropic swelling upon heating and cooling processes. In the following sections, we investigate each thermal-responsive phenomenon of the gels in detail.

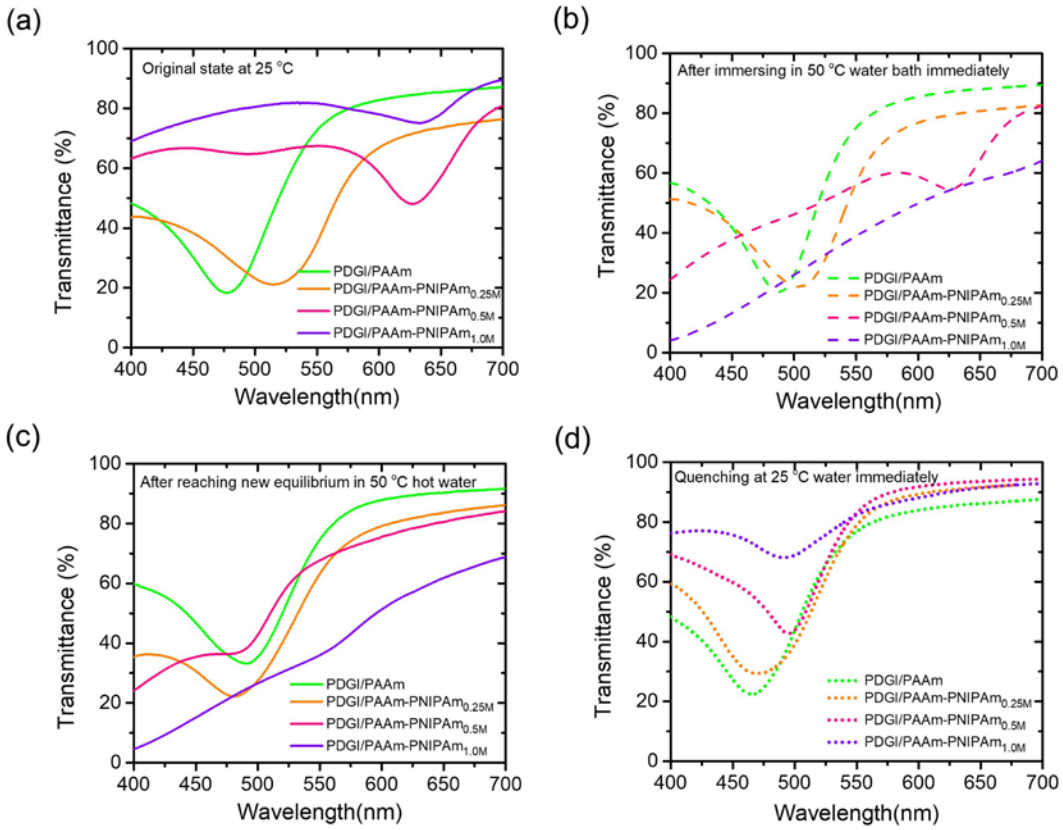

Figure 4. Effect of NIPAM concentration on the turbidity of the PDGI/PAAm-PNIPAM gels. Transmittance of the PDGI/PAAm and PDGI/PAAm-PNIPAM gels with different NIPAM concentrations at (a) original state, (b) after immersing in 50 ℃ water bath immediately, (c) after reaching new equilibrium into 50 ℃ water bath, and (d) quenching state at 25 ℃ water bath after reaching new equilibrium into 50 ℃ water bath. The transmittance was measured immediately after the samples were transferred to the hot or cold bath.

3.4 The effect of NIPAM concentration on turbidity, anisotropic deswelling/reswelling, interplanar distance, and reversibility. The effect of the incorporated PNIPAM density on the ultrafast turbidity transition was investigated. We facilely tuned the turbidity of PDGI/PAAm-PNIPAM hydrogels with the NIPAM concentration, *c*. The transmittance of the PDGI/PAAm and

PDGI/PAAm-PNIPAM gels with different *c* at 25 ℃ is shown in Figure 4a. All the gels exhibited high transmittance. The peaks in the spectra correspond to the structural color. After immersing these gels into a 50 ℃ hot water bath, the transmittance of all the PDGI/PAAm-PNIPAM gels decreased immediately, but the samples with higher *c* showed lower transmittance (Figure 4b). Taken the transmittance at 400 nm as an index, that of the PDGI/PAAm-PNIPAM$_{0.5M}$ gel decreased from 64% to 25%, and that of the PDGI/PAAm-PNIPAM$_{1.0M}$ gel decreased from 69% to 5%. As introduced above, the interpenetration of PNIPAM with PAAm barely affects the phase transition behavior of PNIPAM, but it allows fine-tuning of hydrophobic-hydrophilic balance above LCST. The gels with denser PNIPAM exhibited lower transmittance due to their larger PNIPAM density. Upon this ultrafast transition, the peak wavelength of the spectra, corresponding to the hidden structural color, barely changed. After 2 h immersion in 50 ℃ hot water, the gel reached a new equilibrium at 50 ℃. Upon this long-term deswelling process, the transmittance spectra did not change remarkably but the peak wavelength of the gels exhibited remarkable blue shift, which is in accord with the taken images (Figure 4c and Figure S7).

By quenching the heated shrunken gels into a 25 ℃ cold water bath, the gels recovered their high transmittance immediately (Figure 4d and Figure S7(c)), but the peak wavelength recovered slowly. The peak wavelength of the gels gradually recovered during the long-term reswelling process mainly due to the slow diffusion of water molecules, which is also associated with the time-dependent color change during the cooling process.

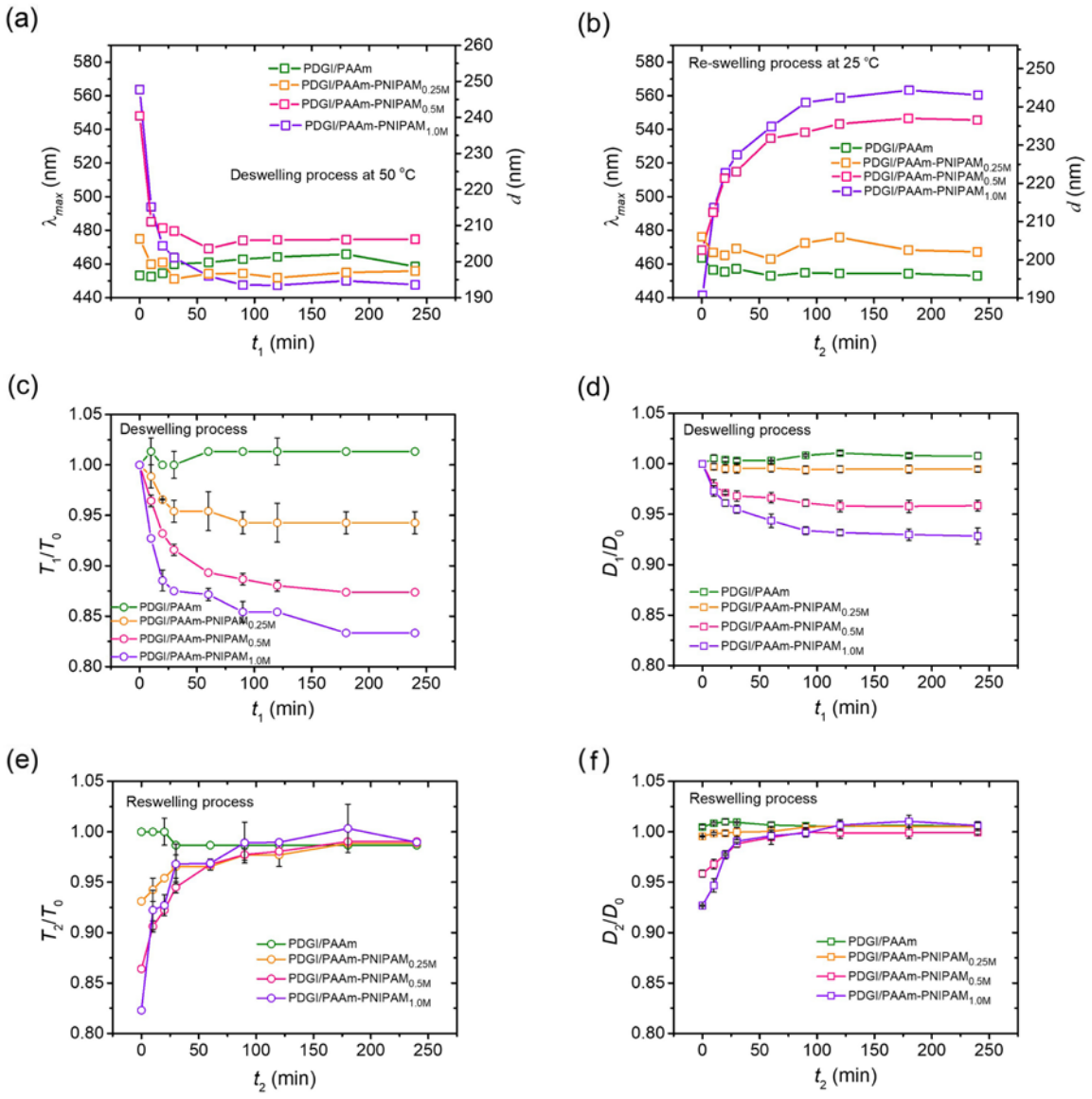

Figure 5. Deswelling and reswelling behaviors of the PDGI/PAAm and PDGI/PAAm-PNIPAM gels with different NIPAM concentrations during the heating and cooling process. λ_{max} of the reflection spectrum and *d* as a function of (a) heating (t_1) and (b) cooling time (t_2); (c,d) deswelling ratios in water as a function of heating time along the thickness : T_1/T_0 (c) and the diameter: D_1/D_0 (d) direction; (e,f) reswelling ratios in water as a function of cooling time along the thickness: T_2/T_0 (e) and the diameter: D_2/D_0 (f) direction compared to original state.

The density of the incorporated PNIPAM networks significantly influences the extent of deswelling and reswelling. PDGI/PAAm-PNIPAM hydrogels exhibit a shift in structural color and the peak wavelength during the heating and cooling process, as revealed by the earlier discussion. To investigate the effect of PNIPAM density on color shift and deswelling/reswelling behavior, the corresponding color and reflection spectra of the PDGI/PAAm-PNIPAM hydrogels with different NIPAM concentration, *c*, during deswelling and reswelling process were collected. The raw data are shown in Figure S8 and S9. Figure 5a and 5b show the change in λ_{max} and *d* for the PDGI/PAAm-PNIPAM hydrogels with different *c* during deswelling and reswelling as a function of t_1 and t_2. The higher *c* was, the greater the extent of the decrease/increase in λ_{max} and *d* during the heating/cooling process became. This indicates that the PNIPAM density in the gels plays a role in the variations of λ_{max} and *d*, which is in accord with the color shift of the gel. It is worth mentioning that the time to reach equilibrium is almost independent of *c* because the timescale is dominated by water diffusion.

The effect of PNIPAM density on the anisotropic deswelling/reswelling is shown in Figure 5c-f. The extent of deswelling/reswelling increased with *c*. On the other hand, swelling anisotropy became less obvious with increasing *c*. PNIPAM is incorporated into the PAAm layer of PDGI/PAAm hydrogels, forming an interpenetrating soft layer of PAAm-PNIPAM within the hydrogels. Such incorporation of the PNIPAM network adds additional osmotic pressure to the gel. At low *c* (0.25 M), incorporating the PNIPAM network leads to negligible swelling of the gels, as a result, the bilayer structure remains intact. Therefore, the gels show negligible in-plane deswelling/reswelling (D_1/D_0 ~ 1.00). With increasing *c*, the addition of PNIPAM networks induces remarkable swelling of the gel layers, which gives tension and damage to the PDGI bilayers. Because of the partial fracture of the PDGI bilayers, the anisotropy in

deswelling/reswelling of the PDGI/PAAm-PNIPAM hydrogels weakens as observed from the slight deswelling along the diameter direction (D_1/D_0 ~ 0.96 for 0.5 M, D_1/D_0 ~ 0.93 for 1.0 M). In addition, the structural color of the gels became less obvious with increasing *c*, which may be attributed to a weaker reflection of light at the bilayer-network interfaces. The reason for the weaker reflection is not clear but might be related to the change in the refractive index of the gel layers after the incorporation of PNIPAM.

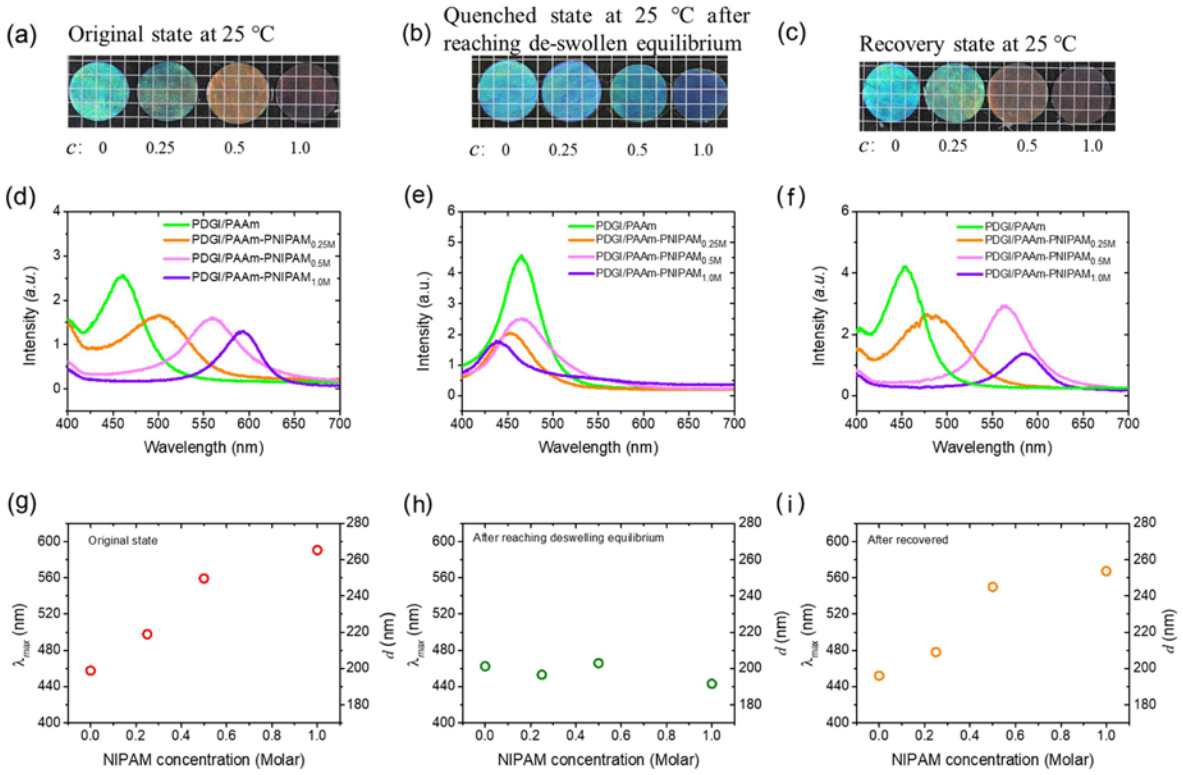

Figure 6. Reversibility in the structural color of the PDGI/PAAm and PDGI/PAAm-PNIPAM gels with different NIPAM concentrations, *c*, during the heating and cooling process. (a-c) Photographs, (d-f) reflection spectra, and (g-i) λ_{max} and *d* as a function of the NIPAM concentration of PDGI/PAAm and PDGI/PAAm-PNIPAM gels with different NIPAM

concentration at original state (a, d, g), deswelling equilibrium state (b, e, h), and recovery state (c, f, i).

To investigate the effect of PNIPAM density on the swelling reversibility of the gel during the heating and cooling process, the photographs and reflection spectra of PDGI/PAAm and PDGI/PAAm-PNIPAM with different *c* after reaching deswelling and reswelling equilibrium are shown in Figure 6. The appearance of the gels at the original state and the deswelling equilibrium state are shown in Figure 6a and 6b, respectively. After the reswelling process, the hydrogels almost recovered the original color (Figure 6c). The reflection spectra of the hydrogels at the original and deswelling equilibrium states are shown in Figure 6d and 6e, respectively. After the reswelling, the reflection spectra of the gels recovered almost completely (Figure 6f). The corresponding λ_{max} and *d* of the gels also exhibited the same trends (Figure 6g–i). These results indicate that the fully reversible color shift of the PDGI/PAAm-PNIPAM gels upon heating-cooling cycles is independent of the PNIPAM density. Consequently, changing the PNIPAM density has a negligible effect on the swelling reversibility of the PDGI/PAAm-PNIPAM gels.

The repeatability of the structural color change of the PDGI/PAAm-PNIPAM hydrogel upon multiple heating-cooling cycles around LCST was further demonstrated (Figure S10). The PDGI/PAAm-PNIPAM$_{0.5M}$ gel recovered to the original color after each heating and cooling process (Figure S10a). The reflection spectra of PDGI/PAAm-PNIPAM$_{0.5M}$ gel after each heating and cooling process around LCST are shown in Figure S10b. The λ_{max} and *d* as functions of a number of recovery times were calculated and are shown in Figure S10c. As can be seen from Figure S10d, the fluctuation of λ_{max} and *d* after each heating and cooling process remained very small (within ±10 nm). It indicates that the gel shows high reversibility in color and lamellar distance after each heating/cooling process. The full width at half maximum (FWHM) of the

reflection spectra of the gel as a function of the number of recovery times also showed negligible fluctuation, which indicates that the properties of the gel barely changed and the gel possesses excellent stability and reversibility. Remarkably, the gel maintained its high turbidity during a one-month immersion in a hot water bath (Figure S10e).

In addition, the gel size (thickness and diameter) upon the multiple cycles also has been investigated to prove the high reversibility (Figure S11). The cycle number does not affect the anisotropic deswelling/reswelling behavior, suggesting that the PDGI/PAAm-PNIPAM$_{0.5M}$ hydrogel exhibits the highly reversible anisotropic swelling behavior.

The drying, UV exposure, and pH tolerance tests for the hybrid hydrogels were also conducted to evaluate the stability, repeatability, and durability of the PDGI/PAAm-PNIPAM hydrogel against harsh conditions. The gel exhibited remarkable stability against the drying and reswelling treatment, and it was unresponsive to both UV exposure and pH change (Figure S13).

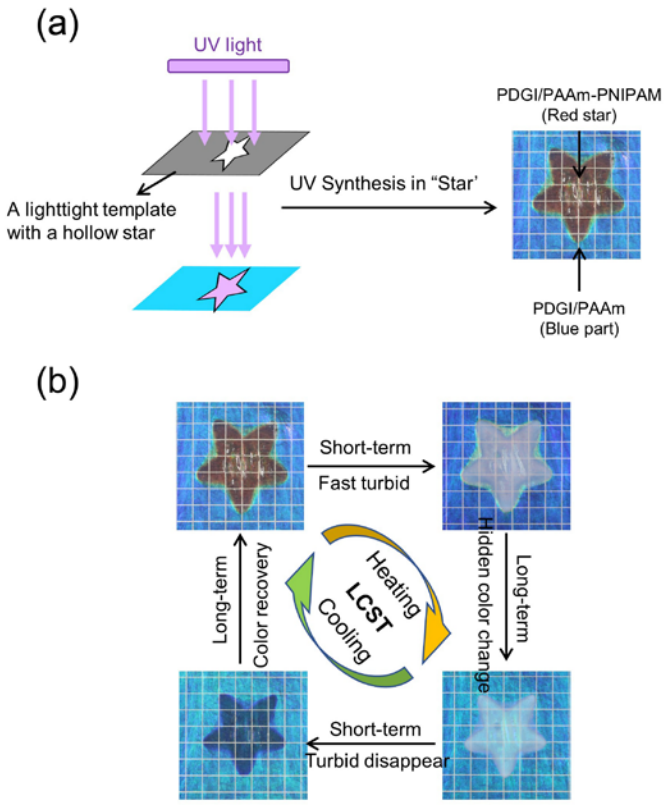

Figure 7. (a) Regioselective synthesis of the thermo-responsive PDGI/PAAm-PNIPAM pattern in the PDGI/PAAm hydrogel and (b) its structural color/turbid transition during heating and cooling process for applications, such as of smart window and smart display. Background lattices: 5 × 5 mm.

3.5 Regioselective incorporation of thermo-responsive component into the anisotropic lamellar hydrogel. The unique ultrafast structural color/turbid transition of the PDGI/PAAm-PNIPAM hydrogels can be potentially applied as smart windows and smart displays that respond to external environments.[2,41-45] Unlike traditional smart window materials that rely on a transparent/turbid transition triggered by temperature changes, the structural color/turbid transition achieved by this work widens the application range of smart window technology, such as for smart stained glass and smart information devices. Toward such applications, we regioselectively

introduced the PNIPAM networks into the PDGI/PAAm lamellar hydrogels by photomasking during UV polymerization. As shown in Figure 7a, the PDGI/PAAm lamellar hydrogel immersed in the NIPAM solution was covered by a photomask with a hollow star, UV-irradiated at 4 ℃ for 8 h, and immersed into pure water. Only the UV-irradiated star area turned red after reaching equilibrium in pure water at *Temp* = 25 ℃, which indicates that the PNIPAM networks can be selectively incorporated into the UV-irradiated area. The structural color/turbid transition of the PDGI/PAAm-PNIPAM hydrogel pattern in the PDGI/PAAm hydrogel is shown in Figure S12 and Figure 7b (right). Upon immersion of the gel into hot water at 50 ℃, the star region immediately got turbid owing to the thermo-induced phase separation of PNIPAM. Like the normal PDGI/PAAm-PNIPAM hydrogels, the star region in the gel exhibited long-term shrinkage with a blue-shift in gel color upon heating and recovery of the structural color upon cooling. This immediate structural color/turbid transition and long-term structural color shift of patterned gel can be applicable to smart stained glass or smart display as follows. At low temperatures, this patterned gel exhibits a mosaic-like structural color reminiscent of stained glass. Conversely, exposure to strong sunlight causes the pattern to cloudy, effectively serving as a smart feature to prevent the rise of the room temperature.

Various temperature-responsive photonic gels have already been reported. Compared to these gels, our PDGI/PAAm-PNIPAM hydrogel has the following advantages and features. Existing photonic gels often have difficulty controlling the structural color in the reference state. In contrast, the structural color of our gel at low temperatures can be controlled in the green-to-red range, depending on the amount of PNIPAM introduced. Wider color control might be achievable through structural modifications of the PDGI/PAAm hydrogels used as templates. Existing temperature-responsive photonic gels often show slow continuous structural color changes in

response to temperature variations. In contrast, our system shows a color/monochrome transition at the LCST of PNIPAM, taking less than 1 s for the change. In addition, temperature-responsive regions can be selectively introduced into this gel to visualize various information. Moreover, the structural color change of our system is reversible and stable. These remarkable attributes of this lamellar gel hold promise for various applications, including drug delivery, smart displays, and smart windows.

4. CONCLUSION

We have successfully synthesized a thermo-responsive photonic PDGI/PAAm-PNIPAM hydrogel with a 2-D lamellar structure. PNIPAM was effectively incorporated into the PAAm soft layer of the PDGI/PAAm lamellar gel base, forming interpenetrating PAAm-PNIPAM layers within the monodomain PDGI bilayers, all while maintaining the anisotropic structure. The gels not only exhibit reversible deswelling/reswelling but also permit structural color, turbidity, and swelling anisotropy tunable by temperature and PNIPAM density. Notably, the gel exhibits ultrafast and reversible structural color/turbid transition around LCST, which represents a unique approach in smart window technology. Moreover, the PNIPAM networks can be regioselectively introduced into the PDGI/PAAm lamellar hydrogels through UV polymerization with photomasking. We believe that this thermo-responsive PNIPAM-based lamellar photonic hydrogel holds great potential for applications in smart windows, sensors, and smart displays.

ASSOCIATED CONTENT

Supporting Information. Differential scanning calorimetry (DSC), turbidity of the hydrogels at different temperatures, effect of temperature and heating time on transmittance, reflection

spectra and visual change of the hydrogels during heating and cooling process, thermo-responsive behavior of PAAm-PNIPAM hydrogels, reversibility test, visual change of PDGI/PAAm-PNIPAM pattern in PDGI/PAAm hydrogel during heating and cooling process (PDF)

Video S1: the behavior of the PDGI/PAAm-PNIPAM$_{0.5M}$ hydrogel at room temperature and 30℃; Video S2: the thermo-responsive behavior of the PDGI/PAAm-PNIPAM$_{0.5M}$ hydrogel at room temperature and 40℃; Video S3: the thermo-responsive behavior of the PDGI/PAAm-PNIPAM$_{0.5M}$ hydrogel at room temperature and 50℃

AUTHOR INFORMATION

Corresponding Author

*Tasuku Nakajima − Institute for Chemical Reaction Design and Discovery (WPI-ICReDD), Hokkaido University, Sapporo 001-0021, Japan; Faculty of Advanced Life Science, Hokkaido University, Sapporo 001-0021, Japan; orcid.org/0000-0002-2235-3478; Email: tasuku @sci.hokudai.ac.jp

*Jian Ping Gong − Institute for Chemical Reaction Design and Discovery (WPI-ICReDD), Hokkaido University, Sapporo 001-0021, Japan; Faculty of Advanced Life Science, Hokkaido University, Sapporo 001-0021, Japan; orcid.org/0000-0003-2228-2750; Email: gong @sci.hokudai.ac.jp

Author

Yang Han − Faculty of Advanced Life Science, Hokkaido University, Sapporo 001-0021, Japan; orcid.org/0000-0002-2235-3478

Yunzhou Guo − Faculty of Advanced Life Science, Hokkaido University, Sapporo 001-0021, Japan; ZJU-Hangzhou Global Scientific and Technological Innovation Center, Zhejiang University, Hangzhou 311215, China; orcid.org/0000-0001-5347-4283

Author Contributions

Y. Han and Y.Z. Guo conceived the idea. Y. Han performed major experiments on the synthesis and modification of gel, deswelling/reswelling behavior, optical measurement, and data analysis and wrote the paper. Y.Z. Guo contributed to the DSC experiment. Y. Han prepared the initial manuscript. T. Nakajima and J. P. Gong supervised the project and edited the manuscript. All authors discussed the results and commented on the manuscript. All authors have approved the final version of the manuscript.

Notes

The authors declare no competing financial interest.

ACKNOWLEDGMENT

This research was supported by JSPS KAKENHI grant numbers 22H04968 and 22K21342. The Institute for Chemical Reaction Design and Discovery (WPI-ICReDD) was established by the World Premier International Research Initiative (WPI), MEXT, Japan. Y. Han thanks the China Scholarship Council (CSC) for financial support during her Ph.D. studies.

REFERENCES

(1) Kim, Y-J.; Matsunaga, Y. T. Thermo-Responsive Polymers and Their Application as Smart Biomaterials. *J. Mater. Chem. B* **2017**, 5, 4307-4321.

(2) Tang, L.; Wang, L.; Yang, X.; Feng, Y.; Li, Y.; Feng, W. Poly(*N*-isopropylacrylamide)-Based Smart Hydrogels: Design, Properties, and Applications. *Prog. Mater. Sci.* **2021**, 115, 100702.

(3) Nagase, K.; Yamato, M.; Kanazawa, H.; Okano, T. Poly(*N*-isopropylacrylamide)-Based Thermoresponsive Surfaces Provide New Types of Biomedical Applications. *Biomaterials* **2018**, 153, 27-48.

(4) Nagase, K.; Okano, T. Thermoresponsive-Polymer-Based Materials for Temperature-Modulated Bioanalysis and Bioseparations. *J. Mater. Chem. B* **2016**, 4, 6381-6397.

(5) Doberenz, F.; Zeng, K.; Willems, C.; Zhang, K.; Groth, T. Thermoresponsive Polymers and Their Biomedical Application in Tissue Engineering - A Review. *J. Mater. Chem. B* **2020**, 8, 607-628.

(6) Ding, Y.; Zhang, X.; Xua, B.; Li, W. LCST and UCST-type Thermoresponsive Behavior in Dendronized Gelatins. *Polym. Chem.* **2022**, 13, 2813-2821.

(7) Keerl, M.; Richtering, W. Synergistic Depression of Volume Phase Transition Temperature in Copolymer Microgels. *Colloid Polym. Sci.* **2006**, 285, 471-474.

(8) Xing, C.; Chen, S.; Liang, X.; Liu, Q.; Qu, M.; Zou, Q.; Li, J.; Tan, H.; Liu, L.; Fan, D.; Zhang, H. Two-Dimensional MXene (Ti_3C_2)-Integrated Cellulose Hydrogels: Toward Smart Three-Dimensional Network Nanoplatforms Exhibiting Light-Induced Swelling and Bimodal Photothermal/Chemotherapy Anticancer Activity. *ACS Appl. Mater. Interfaces* **2018**, 10, 27631-27643.

(9) Novoselov, K. S.; Geim, A. K.; Morozov, S. V.; Jiang, D.; Zhang, Y.; Dubonos, S. V.; Grigorieva, I. V.; Firsov, A. A. Electric Field Effect in Atomically Thin Carbon Films. *Science* **2004**, 306, 666-669.

(10) Sangian, D.; Ide, Y.; Bando, Y.; Rowan, A. E.; Yamauchi, Y. Materials Nanoarchitectonics Using 2D Layered Materials: Recent Developments in the Intercalation Process. *Small* **2018**, 14, 1800551.

(11) Sano, K.; Ishida, Y.; Aida, T. Synthesis of Anisotropic Hydrogels and Their Applications. *Angew. Chem. Int. Ed.* **2018**, 57,2532-2543.

(12) Liu, M.; Ishida, Y.; Ebina, Y.; Sasaki, T.; Hikima, T.; Takata, M.; Aida, T. An Anisotropic Hydrogel with Electrostatic Repulsion between Cofacially Aligned Nanosheets. *Nature* **2015**, 517, 68-72.

(13) Zhao, C.; Zhang, P.; Zhou, J.; Qi, S.; Yamauchi, Y.; Shi, R.; Fang, R.; Ishida, Y.; Wang, S.; Tomsia, A. P.; Liu, M.; Jiang, L. Layered Nanocomposites by Shear-Flow-Induced Alignment of Nanosheets. *Nature* **2020**, 580, 210-215.

(14) Miyamoto, N.; Shintate, M.; Ikeda, S.; Hoshida, Y.; Yamauchi, Y.; Motokawa, R.; Annaka, M. Liquid Crystalline Inorganic Nanosheets for Facile Synthesis of Polymer Hydrogels with Anisotropies in Structure, Optical Property, Swelling/Deswelling, and Ion Transport/Fixation. *Chem. Commun.* **2013**, 49, 1082-1084.

(15) Yang, W.; Yamamoto, S.; Sueyoshi, K.; Inadomi, T.; Kato, R.; Miyamoto, N. Perovskite Nanosheet Hydrogels with Mechanochromic Structural Color. *Angew. Chem. Int. Ed.* **2021**, 133, 8547-8552.

(16) Zhao, Z.; Fang, R.; Rong, Q.; Liu, M. Bioinspired Nanocomposite Hydrogels with Highly Ordered Structures. *Adv. Mater.* **2017**, 29, 1703045.

(17) Le, X.; Lu, W.; Zhang, J.; Chen, T. Recent Progress in Biomimetic Anisotropic Hydrogel Actuators. *Adv. Sci.* **2019**, 6, 1801584.

(18) Haque, M. A.; Kamita, G.; Kurokawa, T.; Tsujii, K.; Gong, J. P. Unidirectional Alignment of Lamellar Bilayer in Hydrogel: One-Dimensional Swelling, Anisotropic Modulus, and Stress/Strain Tunable Structural Color. *Adv. Mater.* **2010**, 22, 5110-5114.

(19) Haque, M. A.; Kurokawa, T.; Kamita, G.; Yue, Y.; Gong, J. P. Rapid and Reversible Tuning of Structural Color of a Hydrogel over the Entire Visible Spectrum by Mechanical Stimulation. *Chem. Mater.* **2011**, 23, 5200-5207.

(20) Yue, Y. F.; Haque, M. A.; Kurokawa, T.; Nakajima, T.; Gong, J. P. Lamellar Hydrogels with High Toughness and Ternary Tunable Photonic Stop-Band. *Adv. Mater.* **2013**, 25, 3106-3110.

(21) Haque, M. A.; Kurokawa, T.; Nakajima, T.; Kamita, G.; Fatema, Z.; Gong, J. P. Surfactant Induced Bilayer-Micelle Transition for Emergence of Functions in Anisotropic Hydrogel. *J. Mater. Chem. B* **2022**, 10, 8386-8397.

(22) Kim, Y. S.; Liu, M.; Ishida, Y.; Ebina, Y.; Osada, M.; Sasaki, T.; Hikima, T.; Takata, M.; Aida, T. Thermoresponsive Actuation Enabled by Permittivity Switching in an Electrostatically Anisotropic Hydrogel. *Nat. Mater.* **2015**, 14, 1002-1007.

(23) Roget, S. A.; Carter-Fenk, K. A.; Fayer, M. D. Water Dynamics in Aqueous Poly-N-Isopropylacrylamide Below and Through the Lower Critical Solution Temperature. *J. Phys. Chem. B* **2022**, 126, 7066-7075.

(24) Ohtsuka, Y.; Sakai, M.; Seki, T.; Ohnuki, R.; Yoshioka, S.; Takeoka, Y. Stimuli-Responsive Structural Colored Gel That Exhibits the Three Primary Colors of Light by Using Multiple Photonic Band Gaps Acquired from Photonic Balls. *ACS Appl. Mater. Interfaces* **2020**, 12, 54127-54137.

(25) Dalier, F.; Dubacheva, G. V.; Coniel, M.; Zanchi, D.; Galtayries, A.; Piel, M.; Marie, E.; Tribet, C. Mixed Copolymer Adlayers Allowing Reversible Thermal Control of Single Cell Aspect Ratio. *ACS Appl. Mater. Interfaces* **2018**, 10, 2253-2258.

(26) Zheng, W. J.; An, N.; Yang, J. H.; Zhou, J.; Chen, Y. M. Tough Al-alginate/Poly(*N*-isopropylacrylamide) Hydrogel with Tunable LCST for Soft Robotics. *ACS Appl. Mater. Interfaces* **2015**, 7, 1758-1764.

(27) Radecki, M.; Spěváček, J.; Zhigunov, A.; Sedláková, Z.; Hanyková, L. Temperature-Induced Phase Transition in Hydrogels of Interpenetrating Networks of Poly(N-Isopropylacrylamide) and Polyacrylamide. *Eur. Polym. J.* **2015**, 68, 68-79.

(28) Chen, X.; Mayama, H.; Matsuo, G.; Torimoto, T.; Ohtani, B.; Tsujii, K. Effect of Ionic Surfactants on the Iridescent Color in Lamellar Liquid Crystalline Phase of a Nonionic Surfactant. *J Colloid Interface Sci.* **2007**, 308-314.

(29) Mito, K.; Haque, M. A.; Nakajima, T.; Uchiumi, M.; Kurokawa, T.; Nonoyama, T.; Gong, J. P. Supramolecular Hydrogels with Multi-Cylindrical Lamellar Bilayers: Swelling-Induced Contraction and Anisotropic Molecular Diffusion. *Polymer* **2017**, 128, 373-378.

(30) Haque, M. A.; Mito, K.; Kurokawa, T.; Nakajima, T.; Nonoyama, T.; Ilyas, M.; Gong, J. P. Tough and Variable-Band-Gap Photonic Hydrogel Displaying Programmable Angle-Dependent Colors. *ACS Omega* **2018**, 3, 55-62.

(31) Na, H.; Kang, Y-W; Park, C. S.; Jung, S.; Kim, H-Y; Sun, J-Y. Hydrogel-Based Strong and Fast Actuators by Electroosmotic Turgor Pressure. *Science* **2022**, 376, 301-307.

(32) Li, X.; Cai, X.; Gao, Y.; Serpe, M. J. Reversible Bidirectional Bending of Hydrogel-Based Bilayer Actuators. *J. Mater. Chem. B* **2017**, 5, 2804-2812.

(33) Harmon, M. E.; Tang, M.; Frank, C. W. A Microfluidic Actuator Based on Thermoresponsive Hydrogels. *Polymer* **2003**, 44, 4547-4556.

(34) Ye, Z.; Sun, S.; Wu, P. Distinct Cation-Anion Interactions in the UCST and LCST Behavior of Polyelectrolyte Complex Aqueous Solutions. *ACS Macro Lett.* **2020**, 9, 974-979.

(35) Asadujjaman, A.; Kent, B.; Bertin, A. Phase Transition and Aggregation Behaviour of an UCST-Type Copolymer Poly-(acrylamide-*co*-acrylonitrile) in Water: Effect of Acrylonitrile Content, Concentration in Solution, Copolymer Chain Length and Presence of Electrolyte. *Soft Matter* **2017**, 13, 658-669.

(36) Li, J.; Ma, Q.; Xu, Y.; Yang, M.; Wu, Q.; Wang, F.; Sun, P. Highly Bidirectional Bendable Actuator Engineered by LCST-UCST Bilayer Hydrogel with Enhanced Interface. *ACS Appl. Mater. Interfaces* **2020**, 12, 55290-55298.

(37) Ding, Y.; Duan, Y.; Yang, F.; Xiong, Y.; Guo, S. High-Transmittance PNIPAm Gel Smart Windows with Lower Response Temperature and Stronger Solar Regulation. *Chem. Eng. J.* **2023**, 460, 141572.

(38) Yue, Y.; Gong, J. P. Structure and Unique Functions of Anisotropic Hydrogels Comprising Uniaxially Aligned Lamellar Bilayers. *Bull. Chem. Soc. Jpn.* **2021**, 94, 2221-2234.

(39) Holz, M.; Heil, S. R.; Sacco, A. Temperature-Dependent Self-Diffusion Coefficients of Water and Six Selected Molecular Liquids for Calibration in Accurate ^{1}H NMRPFG Measurements. *Phys. Chem. Chem. Phys.* **2000**, 2, 4740-4742.

(40) Cui, K.; Yu, C.; Ye, Y. N.; Li, X.; Gong, J. P. Mechanism of Temperature-Induced Asymmetric Swelling and Shrinking Kinetics in Self-Healing Hydrogels. *PNAS* **2022**,119, e2207422119.

(41) Bai, H.; Zhang, Z.; Huo, Y.; Shen, Y.; Qin, M.; Feng, W. Tetradic Double-Network Physical Crosslinking Hydrogels with Synergistic High Stretchable, Self-Healing, Adhesive, and Strain-Sensitive Properties. *J. Mater. Sci. Technol.* **2022**, 98, 169-176.

(42) Yu, Y.; Feng, Y.; Liu, F.; Wang, H.; Yu, H.; Dai, K.; Zheng, G.; Feng, W. Carbon Dots-Based Ultrastretchable and Conductive Hydrogels for High-Performance Tactile Sensors and Self-Powered Electronic Skin. *Small* **2023**, 19, 2204365.

(43) Zhang, Z.; Chen, Z.; Wang, Y.; Chi, J.; Wang, Y.; Zhao, Y. Bioinspired Bilayer Structural Color Hydrogel Actuator with Multienvironment Responsiveness and Survivability. *Small Methods* **2019**, 3, 1900519.

(44) Shao, C.; Yu, Y.; Fan, Q.; Wang, X.; Ye, F. Polyurethane‐Polypyrrole Hybrid Structural Color Films for Dual‐Signal Mechanics Sensing. *Smart Med.* **2022**, 1, e20220008.

(45) Li, X.; Liu, J.; Zhang, X. Pressure/Temperature Dual-Responsive Cellulose Nanocrystal Hydrogels for On-Demand Schemochrome Patterning. *Adv. Funct. Mater.* **2023**, 2306208.

Table of Contents

Incorporation of thermo-responsive PNIPAM into the anisotropic lamellar hydrogels to form an interpenetrating soft layer inside the hydrogels. The hydrogel containing aligned lipid bilayers and thermo-responsive polymers exhibits heat-induced instant color/monochrome transition, structure color modulation, and anisotropic deformation.